V.A.1 Fuel Cell Systems with Low Platinum Loadings

Rajesh K. Ahluwalia (Primary Contact), Xiaohua Wang, Kazuya Tajiri, Romesh Kumar
Argonne National Laboratory
9700 South Cass Avenue
Argonne, IL 60439
Phone: (630) 252-5979
E-mail: walia@anl.gov

DOE Technology Development Manager: Nancy Garland
Phone: (202) 586-5673
E-mail: Nancy.Garland@ee.doe.gov

Project Start Date: October 1, 2003
Project End Date: Project continuation and direction determined annually by DOE

Objectives

- Develop a validated model for automotive fuel cell systems, and use it to assess the status of the technology.
- Conduct studies to improve performance and packaging, to reduce cost, and to identify key research and development issues.
- Compare and assess alternative configurations and systems for transportation and stationary applications.
- Support DOE/FreedomCAR automotive fuel cell development efforts.

Technical Barriers

This project addresses the following technical barriers from the Fuel Cells section of the Fuel Cell Technologies Program Multi-Year Research, Development and Demonstration Plan:

(B) Cost
(C) Performance
(E) System Thermal and Water Management
(F) Air Management
(G) Start-up and Shut-down Time and Energy/Transient Operation

Technical Targets

This project is conducting system level analyses to address the following DOE 2010 and 2015 technical targets for automotive fuel cell power systems operating on direct hydrogen:

- Energy efficiency: 50%-60% (55%-65% for stack) at 100%-25% of rated power
- Power density: 650 W/L for system, 2,000 W/L for stack
- Specific power: 650 W/kg for system, 2,000 W/kg for stack
- Transient response: 1 s from 10% to 90% of rated power
- Start-up time: 30 s from –20°C and 5 s from +20°C ambient temperature
- Precious metal content: 0.3 g/kW (2010), 0.2 g/kW (2015)

Accomplishments

- Determined the performance of nanostructured thin film catalyst (NSTFC) stacks with 0.15 mg/cm^2 Pt loading and supported 20-μm membranes.
- Evaluated the performance of the Honeywell integrated compressor-expander-motor module (CEMM) for 1.5-atm operation.
- Analyzed the performance of parallel ejector-pump hybrids for fuel management.
- Constructed performance maps for planar membrane humidifiers.
- Collaborated with Honeywell to evaluate the performance of advanced microchannel automotive radiators.
- Conducted drive cycle simulations to determine the fuel economy of hybrid fuel cell vehicles for different rated-power efficiencies.

Introduction

While different developers are addressing improvements in individual components and subsystems in automotive fuel cell propulsion systems (i.e., cells, stacks, balance-of-plant components), we are using modeling and analysis to address issues of thermal and water management, design-point and part-load operation, and component-, system-, and vehicle-level efficiencies and fuel economies. Such analyses are essential for effective system integration.

Approach

Two sets of models are being developed. The GCtool software is a stand-alone code with capabilities for design, off-design, steady-state, transient, and constrained optimization analyses of fuel cell systems

(FCS). A companion code, GCtool-ENG, has an alternative set of models with a built-in procedure for translation to the MATLAB/Simulink platform commonly used in vehicle simulation codes such as the Powertrain Systems Analysis Toolkit, commonly known as PSAT.

Results

In Fiscal Year (FY) 2010, we changed our reference FCS configuration (see Figure 1) to eliminate the anode humidifier, switched to a single stack (with metal bipolar plates) that produces the gross power required for 80-kW_e net power, and expanded the system configurations to include the low-pressure option. We evaluated the performance of three systems: S1 – the reference pressurized FCS with 2.5-atm stack pressure at rated power, S2 – a low-pressure FCS with 1.5-atm stack inlet pressure at rated power, and S3, which is S2 without a cathode humidifier [1].

Air Management

We modeled the performance of the Honeywell CEMM originally designed for 2.5-atm peak pressure (S1 conditions). We determined the optimum operating points of the mixed axial flow compressor, variable area nozzle turbine, 3-phase brushless direct current motor, and the liquid-cooled motor controller. We found that the CEMM component efficiencies are quite comparable under S1 and S2 conditions. The main difference is that the peak shaft speed is 85,000 rpm under S2 conditions compared to 110,000 rpm under S1 conditions. Thus, it may be possible to improve the performance of the CEMM for S2 conditions by redesigning it for a higher speed at 1.5-atm and full flow.

Our analysis indicates that the maximum turndown may be limited by compressor surge for shaft speeds less than 45,000 rpm. We estimate that at rated power, the CEMM consumes ~10 kW_e in S1 and <6 kW_e in S2. At idling conditions, the estimated power consumption is 250–400 W_e, depending on the allowable minimum shaft

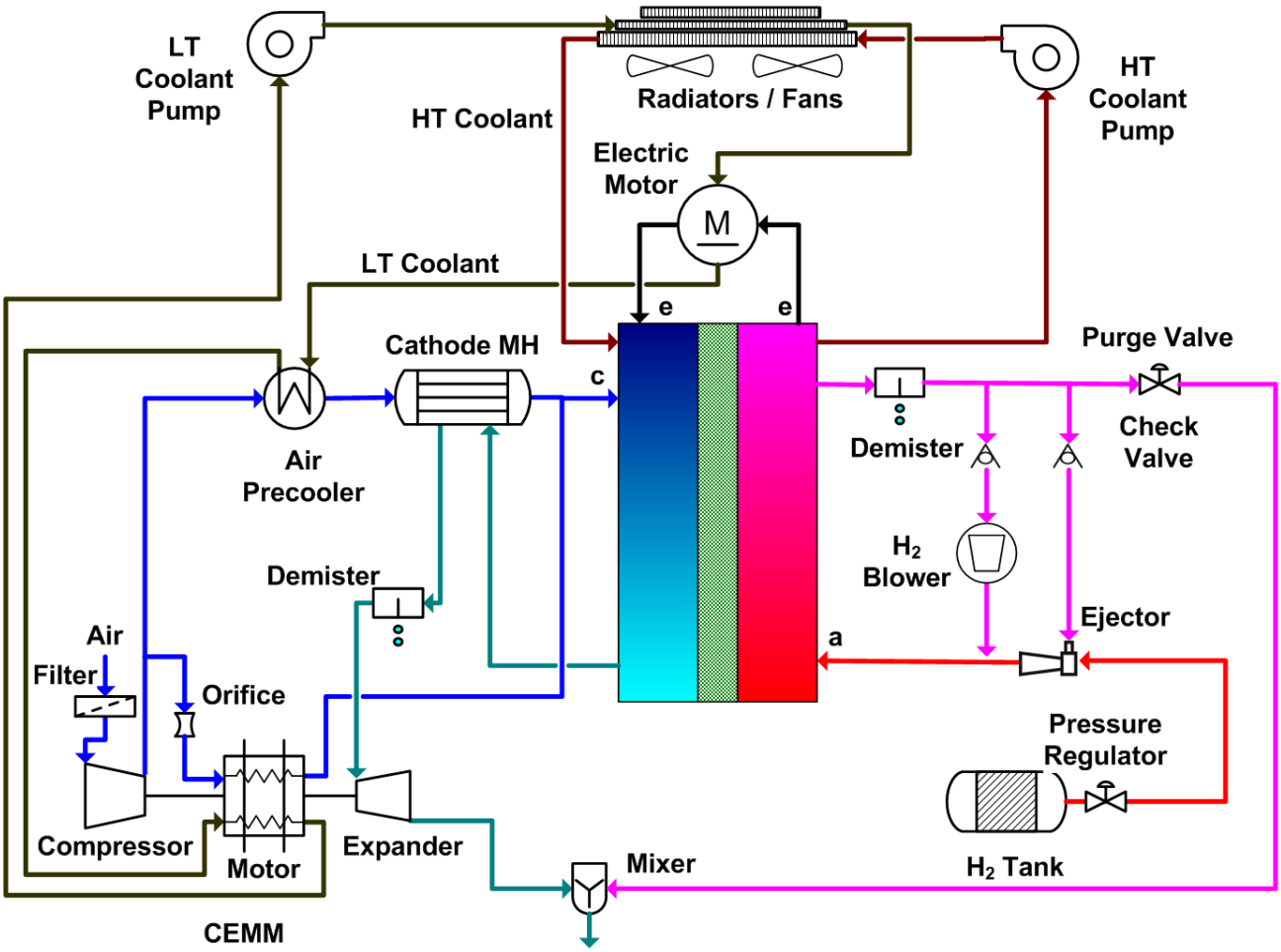

FIGURE 1. Reference Pressurized FCS with Motor Cooling and Membrane Humidifier (MH)
LT - low temperature; HT - high temperature

speed. The minimum shaft speed, if lower than the lift speed, will affect the durability of the airfoil bearings.

Fuel Cell Stack

In FY 2009, we had developed a cell and stack model for 3M's NSTFC-based membrane electrode assemblies (MEAs) using data for electrochemically active surface area, specific activity, short and crossover currents, high-frequency resistance and polarization curves over a wide range of temperatures and inlet relative humidities [2]. In FY 2010, we used the model to determine the optimum stack operating conditions for S1, S2 and S3 scenarios. With fixed air and fuel stoichiometry (50% oxygen and 50% per-pass hydrogen utilization) and rise in coolant temperature (10°C), at rated power, we calculated the optimum stack temperature (i.e., coolant exit temperature) and the inlet cathode and anode dew point temperatures as 85°C/64°C/59°C for S1, 75°C/61°C/53°C for S2, and 65°C/22°C/22°C for S3, respectively. These results clearly show the role of pressurization and air humidification in determining the optimum stack temperature.

Figure 2a shows a comparison of the power density and the Pt content of the FY 2009 (0.1(a)/0.15(c) mg-Pt/cm^2, 35-μm 850 equivalent weight [EW] membrane) and FY 2010 (0.05(a)/0.1(c) mg-Pt/cm^2, 20-μm 850 EW supported membrane) reference S1 systems. We estimate that the power density for the 2010 system is 20% lower at 50% system efficiency due to lower Pt loading (0.8-1 A/cm^2) but is about 6% higher at 40% system efficiency because of the thinner membrane (>2 A/cm^2). Lower Pt loading and thinner membrane combine to produce a 30-45% reduction in Pt content for the 2010 systems (0.12-0.30 g-Pt/kWe-net).

Figure 2b compares the performance of the FY 2010 S1 and S2 systems. The cell voltage in S1 is 25-35 mV higher to achieve the same system efficiency by compensating for the greater CEMM parasitic power. In spite of the higher cell voltage, S1 can have higher power density because of the positive effect of the system pressure on the current density. Depending on the system efficiency, we project up to 12% higher Pt content for the S2 scenario.

Fuel Management

We analyzed the performance of the parallel ejector-pump hybrid in the fuel management system. Figure 3 shows the entrainment by a supersonic ejector [3] in which the motive gas is pure hydrogen from the compressed gas tank and the suction gas is spent hydrogen at the stack outlet. We consider that the motive gas is available at pressure less than 15 atm (regarded as the empty tank pressure) and that the suction gas is saturated with water vapor (molecular weight of 3-7) at 1-1.15 atm (S2 scenario). The desired lift pressure is 3 psi at rated power and the recirculation ratio (suction to primary mass flow rate) is 2-5. In our terminology, entrainment expresses the ratio of the suction flow rate established by the ejector to the flow rate required for 50% hydrogen utilization.

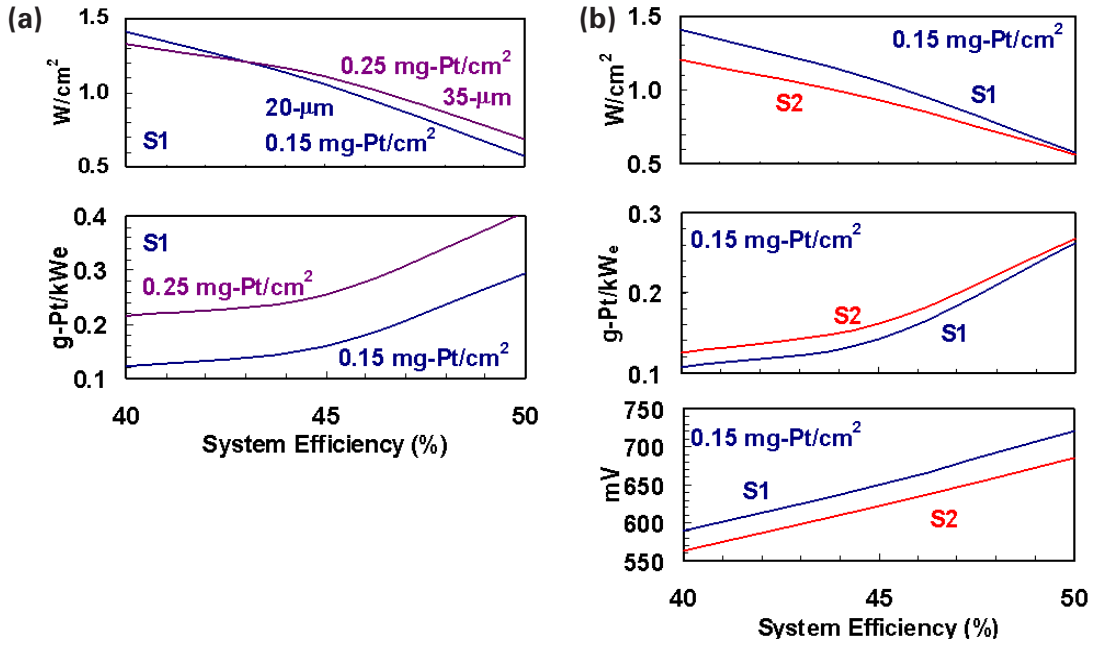

FIGURE 2. Effect of Pt Loading and Stack Operating Pressure on Stack Power Density, Pt Content, and Cell Voltage

Figure 3 shows the entrainment and the motive gas pressure as functions of the normalized stack power. A single ejector alone can recirculate hydrogen for stack power down to 43% of rated power (Figure 3a). Between 28 and 43% stack power, a blower is needed to assist in recirculating the hydrogen; below 28% stack power, the motive gas pressure is too low to achieve the required lift pressure and the blower alone recirculates hydrogen. The ejector-only portion of the operating map can be expanded by including a second ejector that is parallel to and smaller than the first ejector (Figure 3b); however, the blower is still needed for stack power less than 24%. Alternately, a variable throat-area ejector can be employed to expand the ejector-only operating window to 36-100% stack power (Figure 3c).

Our model indicates that, without an ejector, a 400-W (mechanical power) blower is needed to recirculate hydrogen in the S2 scenario. A single fixed-area ejector reduces the blower power by more than 90%. Although the blower power can be reduced considerably with a variable-geometry ejector (to 25 W) or a dual-ejector arrangement (to 10 W), additional complexity may be difficult to justify [4].

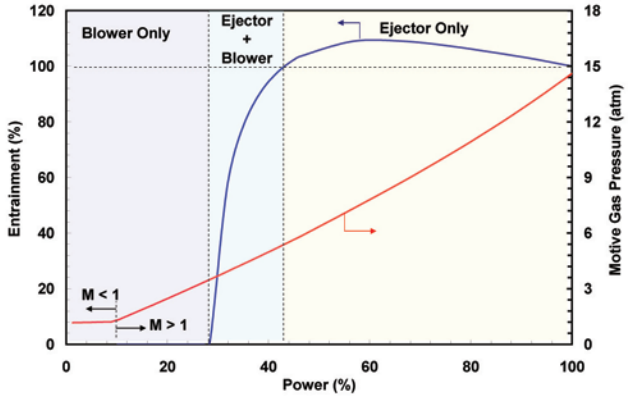

a) Single Ejector and Blower

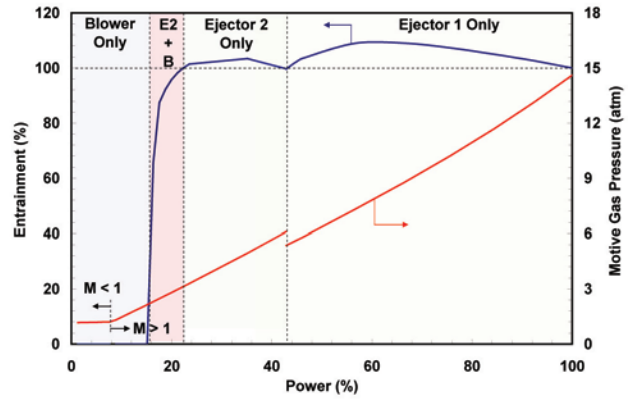

b) Dual Ejectors and Blower

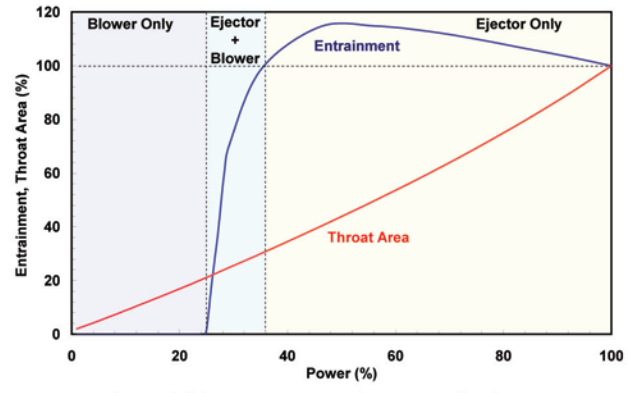

c) Variable-Geometry Ejector and Blower

FIGURE 3. Operating Maps of Ejector-Blower Hybrids

Water Management

We received and analyzed Honeywell and PermaPure data for full-scale, half-scale and one-tenth-scale membrane humidifiers [5]. We derived permeance for the units (aggregate, not local values) and showed that the permeance can be represented in terms of the operating temperatures and the relative humidity of the dry air exiting the humidifier. We also constructed a map for mass-transfer effectiveness factors that, together with the permeance chart, can be used as nomographs for sizing such membrane humidifiers.

We used the data to develop and validate a model to determine the heat and mass transfer between the counterflowing wet and dry streams separated by a Nafion® membrane. The model considers water uptake from the wet stream, diffusion through the Nafion® membrane, and desorption into the dry stream. Figure 4 shows the model results for mass flux of water from a saturated wet stream at 2.5 atm and 80°C to dry air at different inlet temperatures. The flux is a strong function of the dew-point approach temperatures (T_{dp}), the difference between the inlet wet-air T_{dp} and the outlet dry-air T_{dp}. Figure 4 indicates the existence of an

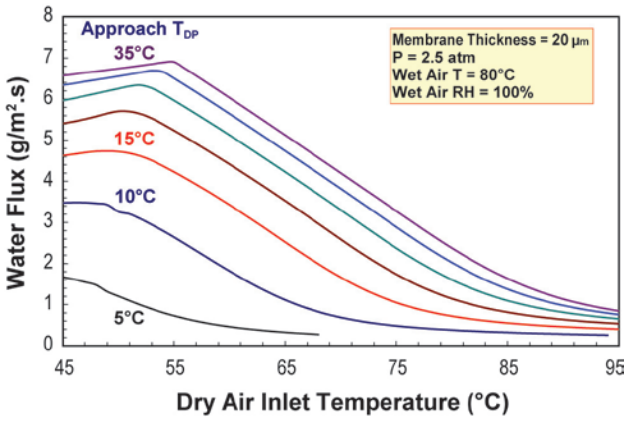

FIGURE 4. Water Mass Transfer Flux in Planar Membrane Humidifier

optimum dry air inlet temperature (T_m) for maximum flux. The flux decreases for dry air inlet temperature (T_d) higher than T_m because of the low water uptake in the membrane (too dry). The flux decreases for T_d lower than T_m because the humidified air approaches saturation. Also, T_m is a function of the dew-point approach temperature. The lower the approach T_{dp}, the lower the T_m, and the smaller is the maximum water flux.

Our simulations show that the water mass transfer flux is also a strong function of the membrane thickness, temperature of the wet air and the operating pressure. For a given approach T_{dp}, the flux increases if the membrane is made thinner, the pressure is increased, or the wet-air temperature (i.e., the stack temperature) is raised.

The results in Figure 4 confirm the importance of including the pre-cooler that lowers the temperature of the compressor discharge air to 55-60°C before entering the humidifier. Without the pre-cooler, the cathode humidifier will need five- to ten-times larger mass-transfer area.

Thermal Management

We received and analyzed the thermal and fluid mechanics data from Honeywell for 23 cm x 23 cm x 3.3 cm sub-scale and 70 cm x 45 cm x 3.3 cm full-scale radiators with 18 and 24 louver fins per inch (fpi) and 40 and 50 fpi plain microchannel fins [5]. We derived the friction factor (*f*) and heat transfer (*j*) coefficients from the data, formulated correlations for the *f* and *j* factors, and incorporated these correlations in our automotive radiator model. We compared the relative performance of the four fin geometries tested and concluded that the 40 fpi microchannel fins are superior to the 18 fpi louver fins in the full-scale design. We also concluded that the fuel cell powertrains may need to be derated for ambient temperatures higher than 40°C since the fan power doubles for every 5°C increase in ambient temperature.

We conducted a study to assess heat rejection in fuel cell vehicles as a function of the FCS efficiency and stack temperature. We considered that the air conditioning condenser (9 kW heat load) and the low-temperature radiator (13-17 kW heat load) are stacked in front of the high-temperature radiator that rejects waste heat generated in the fuel cell stack. Our results show that for a given fan power, the system S2 with 40% efficiency at rated power must be capable of operating at 5-10°C higher stack temperature than the same system with 50% efficiency. Also, from the standpoint of heat rejection, the 40%-efficiency FCS may be acceptable if it can be operated at stack temperatures exceeding 95°C.

We evaluated the prospect of raising the stack temperatures to 95°C under transient conditions (e.g., hill climbing at 55 mph) where high heat rejection may be required for several minutes. We determined that the maximum stack temperature is limited by the system pressure and the dew-point temperature of the cathode air at stack inlet. The CEMM motor power may limit the ability to pressurize adequately if the CEMM does not include an expander. Similarly, the stack temperature cannot be raised if the system does not include a humidifier. We concluded, therefore, that the S3 configuration may not be viable for transportation applications.

System Performance

We analyzed the part-load performance of the S2 system configurations and found that the system efficiencies peak at about 10% of the rated power. Reducing the rated power efficiency from 50% to 45% results in less than a 1% difference in peak efficiency. We also found an inverse relationship between the rated-power efficiency and the system efficiency for power less than 10%; because of hydrogen crossover, the efficiency is marginally higher for the system with 40% rated-power efficiency than the system with 50% rated-power efficiency. We conducted battery-FCS hybrid vehicle simulations to establish the relationship between the rated power efficiency and the system efficiency over drive cycles. The simulations were run for two modes of operation, one in which the FCS is operated primarily as a battery charger and the second in which it is operated in the load-following mode (LFM). The fuel economy is higher in the battery-charging mode (BCM) but the FCS durability may be an issue because of the excessive number of starts and stops. On the Urban Dynamometer Driving Schedule (UDDS), our battery power management strategy produces 58 fuel cell start-stops in BCM and only four in LFM. FCS start-stops can be eliminated altogether if the fuel cell is allowed to idle at low loads. Our LFM simulations indicate that reducing the rated-power efficiency from 50% to 40% results in just 2% difference in system efficiencies over the UDDS, <3% over the Highway Fuel Economy Test (HWFET) cycle, and >9% on the Los Angeles drive cycle (LA92). The corresponding differences in fuel economy are ~2% over the UDDS, <6% over the HWFET, >9% over the LA92, and <7% over the combined cycle used for fuel economy certification. We conclude that reducing the system efficiency at rated power from 50% to 40% results in >50% reduction in Pt content and >40% reduction in cost of stacks manufactured at high volumes while decreasing the peak efficiency by <1% and fuel economy by <7%.

Conclusions and Future Directions

- The variable-area nozzle turbine allows the CEMM to be adapted to different design pressures without significant losses in component efficiencies. The parasitic CEMM power can be reduced by 40% if the compressor discharge pressure is lowered from

2.6 atm (S1 scenario) to 1.6 atm (S2 scenario) at the rated power design point.

- The Pt content can be potentially decreased by 30-45% by reducing the Pt loading from 0.25 mg/cm^2 (2009 status) to 0.15 mg/cm^2 (2010 status) and using a thinner supported membrane (20 μm vs. 35 μm). Depending on the system efficiency at the design point, we project the Pt content (2010 status) to be between 0.12 and 0.30 g/kW$_e$ (net), with the potential to meet the ultimate DOE target.
- Our analysis of the different arrangements of the fuel management system indicates that the recirculation blower power can be decreased by 90% by using a parallel ejector for metering the fuel and entraining the depleted hydrogen from stack outlet. The blower power can be further decreased with dual ejectors or a variable-geometry ejector, but the system complexity may be difficult to justify.
- A pre-cooler between the air compressor and the membrane humidifier can lead to a more than five-fold increase in mass transfer flux of water in the humidifier. Besides the dry air inlet temperature, the water flux is also a strong function of the membrane thickness, temperature of the wet air from the fuel cell stack and the operating pressure.
- From the standpoint of heat rejection, a lower efficiency FCS may be acceptable, provided that the stack temperature can be allowed to increase under certain transient conditions. The maximum stack temperature may be limited by the operating pressure and air humidification.
- In FY 2011, we will investigate the effects of alternative system configurations, rated power efficiency (Pt content) and system operating points on the high-volume manufacturing cost, dynamic drive-cycle performance and component durability.

FY 2010 Publications/Presentations

1. X. Wang, K. Tajiri and R.K. Ahluwalia, "Water Transport during Startup and Shutdown of Polymer Electrolyte Fuel Cell Stacks," Journal of Power Sources, 195 (2010), 6680-6687.

2. K. Tajiri and C.-Y. Wang, "Cold Start of Polymer Electrolyte Fuel Cells," Modern Aspects of Electrochemistry: Modeling and Diagnostics of Polymer Electrolyte Fuel Cells, Ed. by U. Pasagullari and C. Wang, Springer-Verlag, ISBN 0387980679, in press, 2010.

3. R.K. Ahluwalia and X. Wang, "Thermal Management in Automotive Fuel Cell Systems," Fuel Cell Tech Team Meeting USCAR, Southfield, Michigan, April 14, 2010.

4. R.K. Ahluwalia and X. Wang, "Dynamic Behavior of Fuel Hydrogen Impurities in Polymer Electrolyte Fuel Cells," ISO TC197 Working Group 12 Meeting, San Francisco, January 26-29, 2010.

5. R.K. Ahluwalia, X. Wang, B. James, and J. Kalinoski, "Performance and Manufacturing Cost of PEMFC Systems for Automotive Applications," IEA Annex XX Meeting, Rome, Italy, December 16-17, 2009.

6. X. Wang, K. Tajiri and R.K. Ahluwalia, "Startup and Shutdown of Automotive Polymer Electrolyte Fuel Cell Stacks," 2009 Fuel Cell Seminar & Exposition, Palm Springs, California, November 16-19, 2009.

7. R.K. Ahluwalia and X. Wang, "Dynamic Buildup of H_2 Impurities in Anode Recycle Streams of Polymer Electrolyte Fuel Cells," International Workshop on Fuel and Air Quality Issues in Fuel Cells, Berlin, Germany, September 9-11, 2009.

8. X. Wang and R.K. Ahluwalia, "Dynamic Model for Effect of H_2 Impurities on Performance of Polymer Electrolyte Fuel Cells," International Workshop on Fuel and Air Quality Issues in Fuel Cells, Berlin, Germany, September 9–11, 2009.

References

1. R.K. Ahluwalia, X. Wang, K. Tajiri, and R. Kumar, "Fuel Cell Systems Analysis," 2010 DOE Hydrogen Program Review, Washington, D.C., June 8–11, 2010.

2. M.K. Debe, "Advanced Cathode Catalysts and Supports for PEM Fuel Cells," Grant No. DE-FG36-07GO17007, FreedomCAR Tech Team Review, Detroit, MI, March 10, 2010.

3. Y. Zhu, W. Ge, C. Wen, and Y. Li, "Numerical Investigation of Geometry Parameters for Design of High Performance Ejectors," Applied Thermal Engineering, 29 (2009), 898-905.

4. T. Sugawara, S. Kizaki and Y. Nuiya, "Variable Flow Rate Ejector and Fuel Cell System Having the Same," United States Patent, US 6858340, Feb. 22, 2005.

5. Z. Mirza, "Development of Thermal and Water Management System for PEM Fuel Cell," 2010 DOE Hydrogen Program Review, Washington, D.C, June 8–11, 2010.